Metal–Organic Frameworks Hot Paper

International Edition: DOI: 10.1002/anie.201608250
German Edition: DOI: 10.1002/ange.201608250

A Rigid Nested Metal–Organic Framework Featuring a Thermoresponsive Gating Effect Dominated by Counterions

*Qiang Gao[+], Jian Xu[+], Dapeng Cao, Ze Chang, and Xian-He Bu**

Abstract: *We herein report a rigid nested metal–organic framework (MOF) featuring a unique thermoresponsive gating adsorption behavior, which, in contrast to any known flexibility modes for stimuli-responsive MOFs, depends on the thermal motion of the extra-framework counterions. In addition, this MOF also exhibits adsorption selectivity of CO_2 over N_2, H_2, and Ar at 273 K, thus enabling a strategic separation and encapsulation of CO_2.*

Metal–organic frameworks (MOFs) are shown to be good candidates for gas adsorption, separation, and storage, owing to their unique compositional diversity and structural tailorability.[1] Importantly, these features also promise the possibility of integrating some degree of structural transformability into the highly ordered crystalline network. For example, a subclass of MOFs that has the ability to dynamically alter its pore state when subjected to external stimuli (e.g. heat, light, guest adsorption/desorption) has emerged and aroused increasing amounts of interest.[2] With their "smart" stimuli-responsive dynamics, this new generation of MOFs, called "flexible MOFs" or "soft porous crystals", provides more flexibility for many applications.[3] Thus, constructing novel stimuli-responsive MOFs as well as exploring their underlying mechanisms and potential applications are extremely beneficial.[4]

Remarkably, the reported stimuli-responsive MOFs have versatile flexibility modes, including not only breathing and swelling modes, but also linker rotation and subnetwork displacement.[5] Nevertheless, most of these "smart" MOFs have been fabricated only through a deliberate selection of metal nodes and/or organic ligands, because these are the two fundamental units comprising the MOF scaffolds and dominate the underlying framework dynamics in general.[6]

In fact, considering the compositional diversity of MOFs, there may be an alternative way to realize such stimuli-responsive behaviors. It is well established that in most ionic MOFs the counterions, which are indispensable for charge neutrality, are weakly bound to the frameworks via non-covalent interactions.[7] By analogy with the supramolecular assembly, that is, a typical dynamic material involving the rupturing/reforming of non-covalent bonds,[8] this configuration then implies the possibility of applying a certain external stimulus to disturb the fragile non-covalent connections to trigger the dynamics of the extra-framework counterions. Significantly, this feature can enable the stimuli-responsive dynamics of counterions while retaining the integrity of the extended structures, thus realizing the so-called "robust dynamics".[9] In light of this, we report herein an intriguing thermoresponsive MOF, $[Cu_2(BTR)_2]\cdot 2NO_3\cdot x$G (**1**), wherein the NO_3^- ions are of size and shape complementary to, and at low temperatures preferentially locate around, the pores, forming a unique "flask with cork" structure to prevent the entering of guests. More interestingly, these nitrate "corks" exhibit intense motion in response to thermal stimulus, thus capable of regulating a smooth structural transition from closed pore (CP) to open pore (OP) state without compromising the framework robustness.

The single crystal of **1** was synthesized by the solvothermal reaction of $Cu(NO_3)_2\cdot 3H_2O$ and 4,4′-bis(1,2,4-triazole) (BTR) in a binary solvent of water and methanol. The X-ray diffraction analysis reveals that **1** crystallizes in the cubic space group $Fd\bar{3}c$,[10] in which all the Cu^{II} ions were reduced in situ to Cu^{I} (Figure S1 in the Supporting Information). The interactive connection between metal ions and ligands forms the three-dimensional (3D) cationic host framework of **1**, which can be simply identified as a nested structure (Figure 1).[11] The inner "core", denoted as molecular building block 1 (MBB1), is a 0D metal–organic polyhedron (MOP), formed by six Cu1 dimers (Figure S7b) with twelve BTR ligands in octahedral geometry (Figure 1a). Each MBB1 has an overall edge length of approximately 2 nm and involves eight triangle windows of about 4 Å in dimension. Encircling each MBB1 is a much larger confined coordination space, formed by interconnecting twenty-four Cu2 dimers with thirty-six BTR ligands, which, denoted as MBB2, exhibits a distorted truncated octahedral geometry (Figure 1b). Each MBB2 links fourteen adjacent MBB2 in a coplanar packing arrangement to yield a slightly deformed 3D SOD zeolitic outer "shell" (Figure 1c and Figure S8).[12] Note that, each BTR contributes only three N atoms to constructing MBB1 (or MBB2), while the other coordination sites are all

[*] Dr. Q. Gao,[+] Prof. X.-H. Bu
State Key Laboratory of Elemento-Organic Chemistry
College of Chemistry
Nankai University
Tianjin 300071 (P.R. China)
E-mail: buxh@nankai.edu.cn
Dr. Q. Gao,[+] Dr. J. Xu,[+] Dr. Z. Chang, Prof. X.-H. Bu
School of Materials Science and Engineering, TKL of Metal and Molecule-Based Material Chemistry, Collaborative Innovation Center of Chemical Science and Engineering (Tianjin), Nankai University
Tianjin 300350 (P.R. China)
Prof. D. Cao
State Key Lab of Organic-Inorganic Composites
Beijing University of Chemical Technology
Beijing 100029 (P.R. China)
[+] These authors contributed equally to this work.

Supporting information for this article can be found under: http://dx.doi.org/10.1002/anie.201608250.

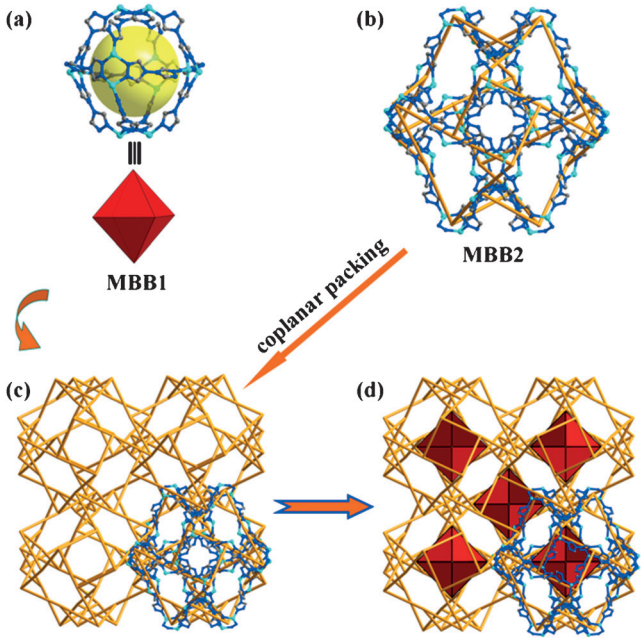

Figure 1. a) MBB1 (the inner "core") with octahedral geometry, b) MBB2, c) The outer "shell" of the nested structure, d) The overall nested host framework of **1**.

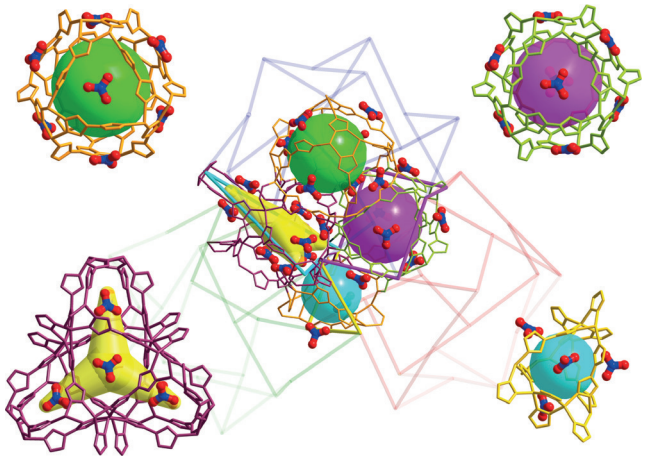

Figure 2. Four types of cages (wire-frame structures, cavities indicated by colored shapes) in **1** with the triangle windows locked by NO_3^- (N dark blue O red).

responsible for interlinking "core" and "shell" (Figure 1 d and Figure S9). The lacunas between "core" and "shell" can be divided into three different types of cages but all with the similar triangle aperture to that of MBB1 (Figure 2).

Overall, the host framework of **1** shows a nested 0D–3D MOP@MOF structure and exhibits a rigid character arising from the coordination mode between copper and BTR ligand. In this structure, the 3D channels with triangle apertures run along the [1 1 1], [−1 1 1], [1 −1 1], and [1 1 −1] directions (Figure S10). From the topological viewpoint, Cu1, Cu2, and two individual BTR ligands can be considered as four different kinds of 4-connected nodes. Thus, the host framework of **1** can be simplified as a 4,4,4,4-connected topological network with the point symbol of $(4_2.6_2.8_2)(4_2.6_3.8)$, which has not yet been reported in literatures (Figure S11).[13] In **1**, the NO_3^- counterions of triangular geometry were transported from the reactant to the framework, which, because of the template effect, are of size and shape complementary to, and at low temperatures captured around, the pores. Thus, the resulting whole framework of **1** can be likened to a "flask with cork" structure (Figure 2). Further, the calculation by PLATON suggests that this framework can provide a guest-accessible volume of about 26135 Å^3 per unit cell (ca. 25.2 % of the total unit cell volume), provided that these "corks" could leave the "flask mouth".[14]

To examine whether the pore phase of **1** is open or closed in the presence of nitrate "corks", we carried out a series of gas adsorption experiments on the activated sample of **1**. The results show that **1** has no obvious sorption of N_2, Ar, H_2, and even CO_2 at low temperatures (Figure 3 and Figure S13), implying the closed pore state of **1** under these conditions. On the other hand, the thermogravimetric analysis (TGA) profile of **1**, however, reveals that the solvent molecules accommodated in the pores were gradually lost in the temperature range of 70–220 °C (Figure S2), thus indicating the "flask mouth" is actually accessible for the leaching of solvents in a wide temperature range.

Note that the activated sample maintained its framework after removal of encapsulated solvents (Figure S3). Therefore, it may seem contradictory that the pores of **1** allow the leaching of solvents but prevent the entering of gas molecules with smaller size. Since temperature is the most significant difference between the TGA and adsorption process, it is then reasonable to presume that this interesting phenomenon is attributed to the distinct pore phases of **1** at different temperatures. To certify this, we then reproduced the gas adsorption experiments at higher temperatures to examine whether or not the pores of **1** could be opened by heat. To calibrate the change in adsorption amount, we chose CO_2 as our test object, because most MOFs usually show a typically higher uptake of CO_2 over other conventional gas molecules under the same conditions. Encouragingly, as Figure 3 illustrates, an abrupt increase in uptake occurred when temper-

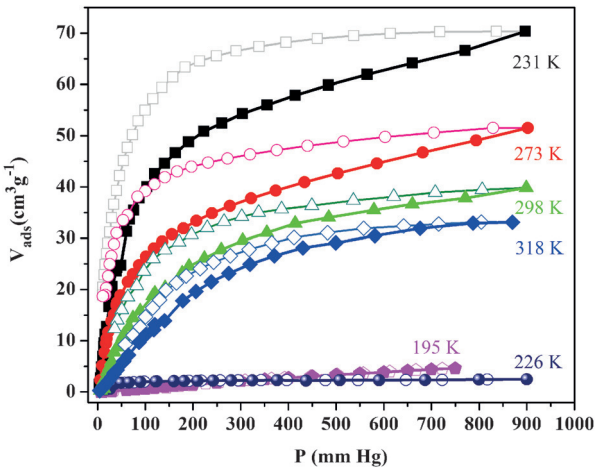

Figure 3. The CO_2 adsorption and desorption isotherms for **1** at different temperatures (1 atm). Filled symbols: adsorption; Open symbols: desorption.

ature approached 231 K (1 atm), referring to the critical threshold beyond which the pores of **1** are dynamically accessible to CO_2 molecules. With temperature further increasing, a monotonous decrease of CO_2 uptake was observed, in agreement with the typical gas adsorption behavior for MOFs, due to the well-known exothermic nature of adsorption process.

Evidently, these results confirm that **1** exhibits a typical gating adsorption behavior in response to ambient temperature change, but an inevitable question arises—what is the key factor at play? Generally, any one of the following factors might be responsible for such a thermoresponsivity, including the kinetics of adsorbates, crystallographic phase transition, thermal expansion effect.[15] To identify the underlying mechanism in this system, we first re-measured the CO_2 sorption isotherm at 195 K with an eight-fold longer equilibrium time. Consequently, there was almost no change in overall uptake (Figure S14). This result not only further confirms the presence of the closed pore state of **1** at low temperatures, but importantly indicates that the kinetics of adsorbates should not be the determining factor for the studied gating phenomenon. Next, we carried out the differential scanning calorimetry (DSC) in the temperature range of 213–323 K. Again, no obvious endothermic and exothermic peaks were observed from the DSC curves (Figure S6a), excluding the presence of the thermal-induced crystallographic phase transition.[4d] In addition, as an indication of the relatively "rigid" nature of the framework, the unit cell parameters of **1** was nearly unchanged after heating (Figure S6b), ruling out the possibility that the observed gating adsorption resulted from thermal expansion. Based on these facts, we perceived that there must be a new stimuli-responsive mode that dictates the thermal-induced gating dynamics of **1**.

Considering the unique "flask with cork" structure of **1**, we then focused our attention on the NO_3^- ions. In fact, the key role of NO_3^- for **1** can be easily verified by examining the adsorption isotherms of the isostructural MOFs with different counteranions. After some setbacks, we finally obtained a new MOF by using the post-synthetic anion exchange method, in which approximately 40 % of NO_3^- was replaced by SCN^-. This new MOF (**1-SCN**) is isostructural to **1** but shows a considerable CO_2 uptake at 195 K (1 atm; Figure S15). This result strongly affirms the decisive role of NO_3^- in controlling the gating adsorption behavior of **1**. Thus, considering the nature of non-covalent interaction between the framework and counterions, we presumed that if the nitrate "corks" could be removed and restored at different temperatures as shown in Figure 4, **1** would then undergo a dynamic structure transition from closed pore to open pore while retaining the framework integrity, which could give rise to the gating adsorption behavior observed experimentally.[3a,c]

To verify this hypothesis, we performed a Grand Canonical Monte Carlo (GCMC) simulation (see details in the Supporting information). Figure S17 shows that the experimental adsorption uptakes of CO_2 at 195 and 273 K quantitatively match with the theoretical values calculated under the closed pore and open pore phase, respectively. This

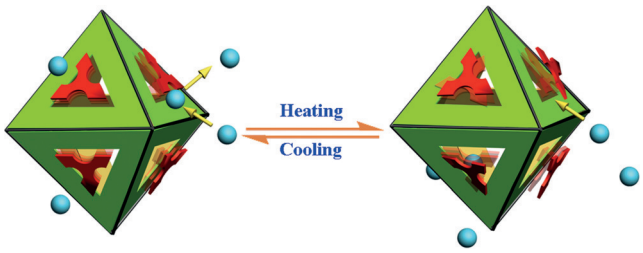

Figure 4. Schematic illustration of the thermoresponsive dynamic behavior of NO_3^- that dictates the gating adsorption of **1**.

satisfactory agreement supports the existence of the open pore and closed pore state in **1** and theoretically supports the structural transition between them at the microscopic scale. Subsequently, we carried out the variable temperature X-ray single-crystal diffraction experiments on the as-synthesized and the activated sample of **1** to monitor the thermodynamics of NO_3^-. In contrast to the negligible metric alteration of the framework, the anisotropic displacement parameters (ADPs) of NO_3^- in the activated sample dramatically increased (see Table S5, Figures S19 and S20), indicative of the intense motion of NO_3^- at high temperatures. As for the as-synthesized sample, a similar phenomenon can also be found when the solvents began to leach from the framework (see Table S5). In addition, we also performed variable-temperature solid-state NMR experiments. From the CP-MAS ^{15}N solid-state NMR spectra of the isotopic labeled sample (**1′**), we found that the characteristic signal of nitrogen displays a dramatic increase in resolution as temperature rises from 253 to 293 K (Figure S21). Such a prominent signal change suggests again that the NO_3^- ions in **1** undergo more intense motion at high temperatures.[16]

Note that the structural transition from closed pore to open pore in **1** should be a smooth process, rather than setting off at a critical temperature. It is easily expected that the thermal motion of NO_3^- should gradually and consistently become more intense as temperature rises, which can be imaged as the thermally excited vibration of the non-covalent bond between NO_3^- and the framework. That would lead to more opportunity for adsorbates to enter, through to the dynamic enlarging of the effective accessible pore size. In this case, the nitrate "corks" would not "permanently" depart from the "flask mouth", that is, there may not be an absolute or static open pore phase to be monitored around the critical temperature, but instead a dynamic pore opening, as illustrated by the results of ADP analysis and NMR spectra. Note that this process is also linked to the kind of adsorbates and their kinetics, owing to the competition between the blocking of NO_3^- and the incoming of adsorbates, as revealed by the gradually increased adsorption rate when temperature raised above 231 K (Table S3).[17]

In addition to thermoresponsivity, **1** also displays a selective adsorption of CO_2 over N_2, H_2, and Ar at 273 K (Figure S16). Then, a strategic separation and encapsulation of CO_2 can be easily implemented by initially loading CO_2 into **1** at 273 K (open "flask" with voids), and subsequently lowering temperature below the threshold to drive the "corks" back onto the "flask mouth" for encapsulation. The

contrast desorption measurement results confirm that the encapsulated amount of CO_2 remained nearly unchanged at the desorption temperature of 210 K, even under a pressure less than 10.5 mmHg, while a considerable amount of CO_2 escaped from the sample at 273 K (Figure S24 and Table S8). From the desorption curve at 210 K, a slight increase in encapsulation amount was observed at the beginning of cooling, which might be due to the hysteresis of structural transition from open pore to closed pore. This experiment thus demonstrates that the quasi-quantitative encapsulation of CO_2 with certain upper limits can be achieved by cooling the sample at different stages of adsorption.

In summary, we report the first example of rigid MOFs featuring the thermoresponsive dynamics based on an entirely new mode. Without causing prominent deformation of the nested structure, a reversible gating adsorption is just realized by thermally triggering the displacement of the NO_3^- "corks" that are of size and shape complementary to the apertures. Thus, this study provides an alternative idea for the design and construction of stimuli-responsive MOFs, which introduces dynamic behavior into MOFs while retaining their structural integrity and robustness.

Acknowledgements

This work was supported by the 973 Program of China (2014CB845600), NNSF of China (21290171, 21421001, 21531005, and 21403116). We thank Prof. Jie-Peng Zhang (Sun Yat-Sen University) for assistance with variable-temperature X-ray single-crystal diffractions, and Profs. Bo Wang (Beijing Institute of Technology), Ping-Chuan Sun (Nankai University) for helpful discussions.

Keywords: counterions · metal–organic frameworks · rigid nested metal–organic framework · robust dynamics · thermoresponsive gating effect

How to cite: *Angew. Chem. Int. Ed.* **2016**, *55*, 15027–15030
Angew. Chem. **2016**, *128*, 15251–15254

[1] a) H. Furukawa, N. Ko, Y. B. Go, N. Aratani, S. B. Choi, E. Choi, A. Q. Yazaydin, R. Q. Snurr, M. O'Keeffe, J. Kim, O. M. Yaghi, *Science* **2010**, *329*, 424–427; b) W. Lu, Z. Wei, Z.-Y. Gu, T.-F. Liu, J. Park, J. Park, J. Tian, M. Zhang, Q. Zhang, T. Gentle, M. Bosch, H.-C. Zhou, *Chem. Soc. Rev.* **2014**, *43*, 5561–5593; c) V. Guillerm, L. J. Weselinski, Y. Belmabkhout, A. J. Cairns, V. D'Elia, L. Wojtas, K. Adil, M. Eddaoudi, *Nat. Chem.* **2014**, *6*, 673–680; d) P. Nugent, Y. Belmabkhout, S. D. Burd, A. J. Cairns, R. Luebke, K. Forrest, T. Pham, S.-Q. Ma, B. Space, L. Wojtas, M. Eddaoudi, M. J. Zaworotko, *Nature* **2013**, *495*, 80–84.

[2] a) S. Kitagawa, M. Kondo, *Bull. Chem. Soc. Jpn.* **1998**, *71*, 1739–1753; b) S. Horike, S. Shimomura, S. Kitagawa, *Nat. Chem.* **2009**, *1*, 695–704; c) G. Férey, C. Serre, *Chem. Soc. Rev.* **2009**, *38*, 1380–1399; d) A. Schneemann, V. Bon, I. Schwedler, I. Senkovska, S. Kaskel, R. A. Fischer, *Chem. Soc. Rev.* **2014**, *43*, 6062–6096; e) C. Serre, C. Mellot-Draznieks, S. Surblé, N. Audebrand, Y. Filinchuk, G. Férey, *Science* **2007**, *315*, 1828–1831; f) C. R. Murdock, B. C. Hughes, Z. Lu, D. M. Jenkins, *Coord. Chem. Rev.* **2014**, *258*, 119–136.

[3] a) S. Q. Ma, D.-F. Sun, X.-S. Wang, H.-C. Zhou, *Angew. Chem. Int. Ed.* **2007**, *46*, 2458–2462; *Angew. Chem.* **2007**, *119*, 2510–2514; b) J. P. Zhang, X.-M. Chen, *J. Am. Chem. Soc.* **2008**, *130*, 6010–6017; c) S. Q. Ma, D.-F. Sun, D.-Q. Yuan, X.-S. Wang, H.-C. Zhou, *J. Am. Chem. Soc.* **2009**, *131*, 6445–6451; d) L. Hamon, P. L. Llewellyn, T. Devic, A. Ghoufi, G. Clet, V. Guillerm, G. D. Pirngruber, G. Maurin, C. Serre, G. Driver, W. Beek, E. Jolimaître, A. Vimont, M. Daturi, G. Férey, *J. Am. Chem. Soc.* **2009**, *131*, 17490–17499; e) R. Matsuda, T. Tsujino, H. Sato, Y. Kubota, K. Morishige, M. Takata, S. Kitagawa, *Chem. Sci.* **2010**, *1*, 315–321.

[4] a) M. T. Wharmby, S. Henke, T. D. Bennett, S. R. Bajpe, I. Schwedler, S. P. Thompson, F. Gozzo, P. Simoncic, C. Mellot-Draznieks, H.-Z. Tao, Y.-Z. Yue, A. K. Cheetham, *Angew. Chem. Int. Ed.* **2015**, *54*, 6447–6451; *Angew. Chem.* **2015**, *127*, 6547–6551; b) F.-X. Coudert, *Chem. Mater.* **2015**, *27*, 1905–1916; c) I. Schwedler, S. Henke, M. T. Wharmby, S. R. Bajpe, A. K. Cheetham, R. A. Fischer, *Dalton Trans.* **2016**, *45*, 4230–4241; d) F. Salles, A. Ghoufi, G. Maurin, R. G. Bell, C. Mellot-Draznieks, G. Férey, *Angew. Chem. Int. Ed.* **2008**, *47*, 8487–8491; *Angew. Chem.* **2008**, *120*, 8615–8619.

[5] a) D. Bousquet, F.-X. Coudert, A. G. Fossati, A. V. Neimark, A. H. Fuchs, A. Boutin, *J. Chem. Phys.* **2013**, *138*, 174706; b) F.-X. Coudert, A. Boutin, A. H. Fuchs, A. V. Neimark, *J. Phys. Chem. Lett.* **2013**, *4*, 3198–3205.

[6] a) S. Henke, A. Schneemann, A. Wütscher, R. A. Fischer, *J. Am. Chem. Soc.* **2012**, *134*, 9464–9474; b) S. B. Choi, H. Furukawa, H. J. Nam, D. Y. Jung, Y. H. Jhon, A. Walton, D. Book, M. O'Keeffe, O. M. Yaghi, J. Kim, *Angew. Chem. Int. Ed.* **2012**, *51*, 8791–8795; *Angew. Chem.* **2012**, *124*, 8921–8925.

[7] A. Karmakar, A. V. Desai, S. K. Ghosh, *Coord. Chem. Rev.* **2016**, *307*, 313–341.

[8] a) X.-Z. Yan, F. Wang, B. Zheng, F.-H. Huang, *Chem. Soc. Rev.* **2012**, *41*, 6042–6065; b) X. Ma, H. Tian, *Acc. Chem. Res.* **2014**, *47*, 1971–1981.

[9] H. X. Deng, M. A. Olson, J. F. Stoddart, O. M. Yaghi, *Nat. Chem.* **2010**, *2*, 439–443.

[10] Crystal data for **1** ($C_8H_8Cu_2N_{14}O_6$): $M_r = 523.38$, cubic, Space group $Fd\bar{3}c$, $a = 47.0072(3)$ Å, $Z = 192$, $R1 = 0.0409$, $wR2 = 0.1250$ and GOF = 1.115. CCDC 1029711 contains the supplementary crystallographic data for this paper. These data can be obtained free of charge from The Cambridge Crystallographic Data Centre.

[11] a) F. Bu, Q. P. Lin, Q.-G. Zhai, L. Wang, T. Wu, S.-T. Zheng, X. H. Bu, P. Y. Feng, *Angew. Chem. Int. Ed.* **2012**, *51*, 8538–8541; *Angew. Chem.* **2012**, *124*, 8666–8669; b) D. Tian, Q. Chen, Y. Li, Y.-H. Zhang, Z. Chang, X.-H. Bu, *Angew. Chem. Int. Ed.* **2014**, *53*, 837–841; *Angew. Chem.* **2014**, *126*, 856–860.

[12] a) C. Baerlocher, W. M. Meier, D. H. Olson, *Atlas of Zeolite Framework Types*, 5th ed, Elsevier, Amsterdam, **2001**; b) K. S. Park, Z. Ni, A. P. Côté, J. Y. Choi, R.-D. Huang, F. J. Uribe-Romo, H. K. Chae, M. O'Keeffe, O. M. Yaghi, *Proc. Natl. Acad. Sci. USA* **2006**, *103*, 10186–10191.

[13] V. A. Blatov, A. P. Shevchenko, D. M. Proserpio, *Cryst. Growth Des.* **2014**, *14*, 3576–3586.

[14] A. L. Spek, *J. Appl. Crystallogr.* **2003**, *36*, 7–13.

[15] D. Zhao, D. Q. Yuan, R. Krishna, J. M. Baten, H.-C. Zhou, *Chem. Commun.* **2010**, *46*, 7352–7354.

[16] a) V. N. Vukotic, K. J. Harris, K. L. Zhu, R. W. Schurko, S. J. Loeb, *Nat. Chem.* **2012**, *4*, 456–460; b) X. Q. Hou, R. J. Kirkpatrick, P. Yu, D. Moore, Y. Kim, *Am. Mineral.* **2000**, *85*, 173–179.

[17] H. Kim, D. G. Samsonenko, M. Yoon, J. W. Yoon, Y. K. Hwang, J.-S. Chang, K. Kim, *Chem. Commun.* **2008**, 4697–4699.

Received: August 23, 2016
Published online: October 28, 2016

